

# ANISOTROPIC PRE-STACK DEPTH MIGRATION OF SEISMIC DATA: A CASE STUDY IN SOUTHWEST OF IRAN

EBRAHIM ZARE<sup>1</sup>, MOHAMMAD ALI RIAHI<sup>2\*</sup>, MAHDI NAZARI SAREM<sup>3</sup>

<sup>1</sup>*Petroleum, Mining and Materials Engineering, Islamic Azad University, Central Tehran Branch, Tehran, Iran.*

<sup>2</sup>*Institute of Geophysics University of Tehran, Iran (\*Corresponding author, Email: maria-hi@ut.ac.ir)*

<sup>3</sup>*Petroleum, Mining and Materials Engineering, Islamic Azad University, Central Tehran Branch, Tehran, Iran.*

(Received January 18, 2024; revised version accepted September 03, 2024)

## ABSTRACT

Pre-stack depth migration (PSDM) is a well-known tool for dealing with lateral velocity changes and complex structures. Considering anisotropy in PSDM is particularly important where a significant velocity variation with direction results in inaccurate move correction and erroneous well-tie. Anisotropic PSDM (APSDM) corrects the mispositioning of events and alleviates the hockey sticks on common-depth-point (CDP) gathers due to the anisotropy. In this study, we incorporated anisotropy into the Kirchhoff PSDM of seismic data recorded in Abadan Plain, southwestern Iran. The true depth of the horizons (Markers) of the Well AY1 are used to calculate anisotropic parameters before the APSDM. The results are verified using the markers of another well (Well BZ1). The results of applying the APSDM in the Abadan Plain make this method efficient in correcting the miss position events and addressing the hockey sticks on CDP gathers while ensuring correct subsurface positioning of horizons in the zero-offset section

**KEY WORDS:** Anisotropy, APSDM, Hockey-sticks, Pre-Stack, Thomson's parameters

## INTRODUCTION

Achieving a correct and realistic subsurface image is the goal of seismic processing. As a major tool for achieving this goal, seismic data migration seeks to migrate dipping reflections to their correct subsurface positions and collapse the so-called seismic diffraction energy to the corresponding scattering points. Indeed, the final output of the migration is supposed to be a section that resembles, as closely as possible, the real geologic cross-section along the seismic line (Yilmaz, 2001). Pre-stack depth migration (PSDM) is the method of choice when encountering strong lateral velocity variations along with complex structures. The Kirchhoff migration (Schneider, 1978) has long been a popular technique for applying PSDM.

In conventional PSDM, it is assumed that seismic velocity does not vary with direction and the medium is isotropic. However, the fact is that the earth is geologically complex and anisotropic, implying that seismic velocity varies with direction (Thomsen, 2014). So, reaching a realistic subsurface image with correct positions of events is virtually impossible unless anisotropic assumptions are taken when practicing seismic data migration.

For an anisotropic medium, the conventional normal moveout (NMO) equation produces inaccurate results at far offsets. For any offset exceeding the target reflector depth, the difference between conventional hyperbolic moveout approximation and the real traveltimes is so significant that hockey-stick events appear on the produced section. In addition, shallower reflectors at longer offsets are stretched upon conventional NMO correction (Abedi et al., 2019). In this case, stacking of traces corresponding to all offsets produces a noisy section in which reflectors cannot be identified properly. In conventional processing, this problem is addressed by muting the shallow parts of the traces corresponding to far offsets to achieve continuous reflectors (especially in the shallower part) and a noise-free section. Given that such a process tends to kill part of the otherwise available data, one may alternatively incorporate the anisotropy into the NMO equation. Several equations have been developed for nonhyperbolic traveltimes approximation in transversely isotropic media with vertical symmetry axis (vertical transverse isotropy, VTI) (*e.g.*, rational approximation (Tsvankin, 1994; Tsvankin & Thomsen, 1994), generalized moveout approximation (Stovas & Fomel, 2017).

Ignorance of anisotropy in transversely isotropic media can set the scene for the PSDM to mislead subsurface imaging, ending up with, for example, mispositioning errors (Alkhalifah & Larner, 1994; Isaac & Lawton, 1999).

The main objective of this paper is to correct the miss position events and address the hockey sticks on CDP gathers while ensuring correct subsurface positioning of horizons in the zero-offset section by implication of the anisotropy into the Kirchhoff PSDM of seismic data recorded in Abadan Plain. Here, we consider the VTI in the migration stage. A comparison of the results of anisotropic

and isotropic approaches to PSDM against wellbore markers indicates that the anisotropic PSDM (APSDM) can properly correct the mispositioning of events while attenuating the hockey stick events on CDP gathers. It is worth noting that the APSDM method has not been previously applied in the area of study which makes this work different from previous studies (e.g., Kianoush et al., 2023).

## GEOLOGICAL SETTING

This study is based on seismic reflection data acquired across Abadan Plain, southwestern Iran. The plain is delineated by the Zagros Fault-Thrust Belt in the north and has been recognized as a part of the Mesopotamian Basin in Iran. The majority of structures in this area follow the structural characteristics of the Arabian Plate. The Arabian-Eurasian plate collision in the Late Eocene has caused the formation of the Zagros highs, northwestward bending of the northern part of the anticlines within the Abadan Plain, and gentle dip of some structures to the north.

## MATERIALS AND METHODS

### Data

Two sets of data were used in this work, namely well data and seismic reflection data. The seismic data was acquired with the acquisition parameters presented in Table 1. The well data came from two wells that were previously drilled in the study area and subjected to a variety of geological and geophysical tests. Accordingly, VSP data and geological stratigraphic sequences were available, making it possible to undertake not only well tying but also correlating different horizons between well and seismic data to calculate initial anisotropy parameters. A location map of the study area is shown in Fig. 1. Used to calculate initial anisotropy parameters and study the heterogeneity of the anisotropy parameters, Wells AY1 and BZ1 are located at a distance of 95 and 185 m to the seismic line, respectively. Selecting wells close to the seismic line has the benefit of reducing the error of computing the anisotropic parameters.



Figure 1. Location and elevation contour map of the study area showing the seismic line (Red line) and Wells AY1 (green circle) and BZ1 (red circle).

Table 1. Acquisition parameters for the studied seismic data.

Source interval	Receiver interval	No. of active channels	Nominal fold
30 m	10 m	720	120

## Pre-processing

The pre-processing (i.e., all processing steps prior to actual PSDM) was done based on a standard processing sequence to enhance the signal-to-noise ratio (SNR). To this end, every shot gather was checked visually, and dead or very noisy traces were killed manually. Necessary amplitude corrections (e.g., spherical divergence, attenuation, surface-consistent amplitude correction) were applied to the data. Spiking deconvolution was performed with an operator length of 150 ms to increase the frequency bandwidth of the data. Fig. 2a shows a typical raw shot gather from one of the southernmost shot points on the seismic line, on which several reflections can be identified. Fig. 2b shows the same shot gather after the processing sequence described in Table 2. The reflections stand out much clearer and can be traced over the entire offset range together with additional previously obscured reflections that were not directly visible in the raw shot gather.

Table 2. Sequential pre-processing steps.

### Stages

- ☐ Trace editing (manual)
- ☐ Static correction (refraction tomography)
- ☐ Denoising (FK-based and band-pass filtering)
- ☐ Surface-consistent amplitude correction
- ☐ Deconvolution
- ☐ Residual static correction

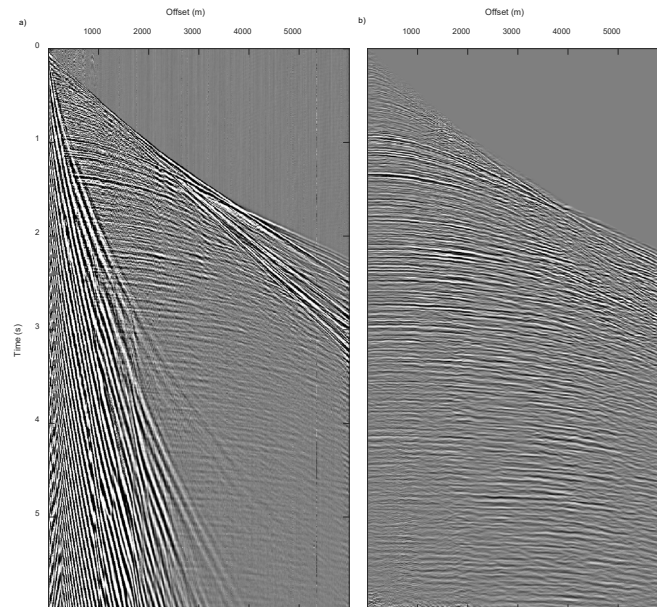


Figure 2. A seismic shot gather prior to PSDM: (a) raw shot gather, and (b) pre-processed shot gather.

## Anisotropic velocity model

A requirement for any PSDM process is the seismic velocity. The process begins with an initial velocity model and updates it iteratively, and the reliability of subsurface imaging is highly dependent on the initial velocity model. In this study, the output velocity model from the pre-stack time migration (PSTM) was used as a basis to build the initial velocity model for the PSDM. First, the obtained RMS velocity obtained from the PSTM was converted to instantaneous velocity using the Dix equation. Initially obtained as a function of depth for every 50 CDPs, the instantaneous velocities were propagated to an instantaneous velocity section covering every single CDP. Afterward, the section was smoothed and used as the initial velocity model for PSDM.

## Anisotropic Kirchhoff PSDM

The compelling reason for doing depth migration is to adequately capture the effect of lateral velocity variations. Pre-stacking nature of the PSDM is, however, necessary to account for nonhyperbolic moveouts caused by lateral velocity variations. In a strict theoretical sense, in the presence of lateral velocity variations, you need to image the subsurface by migration of seismic data in depth, before stacking (Yilmaz, 2001). In fact, backpropagation of the wavefield by migration can provide us with the correct position of seismic reflections in depth. So, this section deals with the theory of PSDM briefly.

Since the Kirchhoff PSDM is usually implemented as a weighted stack of the traveltimes isochrones, traveltimes information for shot and receiver positions is required to construct the diffraction surfaces. In this study, traveltimes values were calculated using the wavefront reconstruction method, which is based on ray tracing on a grid where a fan of rays is transmitted from the source/receiver position to a set of subsurface points lying within the predefined aperture (Vinje, Iversen, & Gjoystdal, 1993). When it comes to an anisotropic, rather than an isotropic, medium (VTI in this study), one must change particular parameters of the stiffness matrix as well as the employed traveltimes equation as follows.

For a VTI medium, stiffness matrix parameters can be expressed with Thomsen's (1986) anisotropy parameters (Thomsen, 1986):

$$\varepsilon = \frac{C_{11} - C_{33}}{2C_{33}} \quad (1)$$

$$\delta = \frac{(C_{13} + C_{44})^2 - (C_{33} - C_{44})^2}{2C_{33}(C_{33} - C_{44})} \quad (2)$$

In which  $C_{11}$ ,  $C_{33}$ ,  $C_{13}$  and,  $C_{44}$  are the elements of the stiffness matrix. The dimensionless parameters  $\varepsilon$  and  $\delta$  (*i.e.*, Thomson's parameters) describe the deviation of the anisotropic traveltimes isochrone from the respective isotropic

traveltime isochrone, implying that they vanish for an isotropic medium. Considering traveltime, Alkhalifah and Tsvankin (1995) proposed the following equation for VTI media and large-offset acquisition (Alkhalifah & Tsvankin, 1995):

$$t^2 = t_0^2 + \frac{x^2}{v^2} + \frac{2\eta x^4}{v^2[t_0^2 v^2 + (1 + 2\eta)x^2]} \quad (3)$$

where  $\eta$  is called the anellipticity parameter and expressed as below:

$$\eta = \frac{\varepsilon - \delta}{1 + 2\delta} \quad (4)$$

While  $\eta$  provides a full scope for time-domain anisotropic processing, the availability of  $\eta$  and/or  $\varepsilon$  is insufficient for depth-domain imaging. For that,  $\delta$  has to be computed from well data (Al-Chalabi, 2014), as follows:

$$\delta_n = \frac{1}{2} \left[ \left( \frac{\Delta z_{seismic,n}}{\Delta z_{marker,n}} \right)^2 - 1 \right] \quad (5)$$

in which the subscript  $n$  refers to the  $n$ th layer.  $\Delta z_{seismic,n}$  and  $\Delta z_{marker,n}$  are the thickness of the  $n$ th formation measured through seismic depth imaging and well tops data, respectively. To start APSDM, one should begin with elliptical anisotropy (*i.e.*,  $\delta = \varepsilon$ ) and then update Thomson's parameters through tomography. So, the initial value for  $\delta$  is obtained from well tops data and the initial  $\varepsilon$  is set to  $\delta$  if it is positive and 0 otherwise.

## RESULTS

This section presents the results of calculating Thomson's parameters from well data followed by the comparison of isotropic and anisotropic results.

### Well markers and the values of $\varepsilon$ and $\delta$

The initial values of  $\delta$  were obtained from check-shot data along Well AY1, as shown in Fig. 3. The nearest CDP on the seismic line to the Well AY1 is CDP No. 5798. At this well, the well tops do not coincide with the tops of imaged horizons through PSDM, showing 56, 37, 76, and 72 m of depth mismatch for Gs, As, Pd, and Kz horizons, respectively. These deviations in depth were employed to set the initial  $\delta$  values. On the other hand, the initial  $\varepsilon$  values were set to  $\delta$ , as explained in Section 3.4. Accordingly,  $\delta$  and  $\varepsilon$  sections (Figs. 4 and 5, respectively) were assumed to remain unchanged between successive horizons. These sections were updated afterward using tomography. The updated the  $\delta$  section became smoother along the horizons (Fig. 4d), with the lowest part of  $\delta$  section being extended from the CDP No. 6200 to the CDP No. 6400 (Fig. 4d). Similarly, starting from the initial  $\varepsilon$  section and updating the section (Fig. 5a), the horizons got smoother (Fig. 5d).



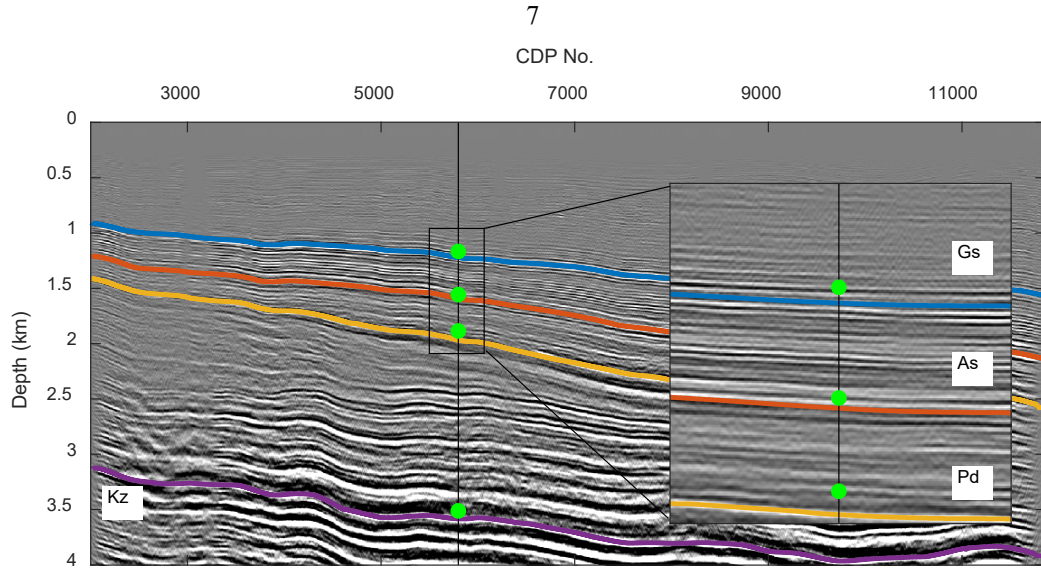


Figure 3. Isotropic PSDM stack with horizons and well tops along Well AY1 (green circles).

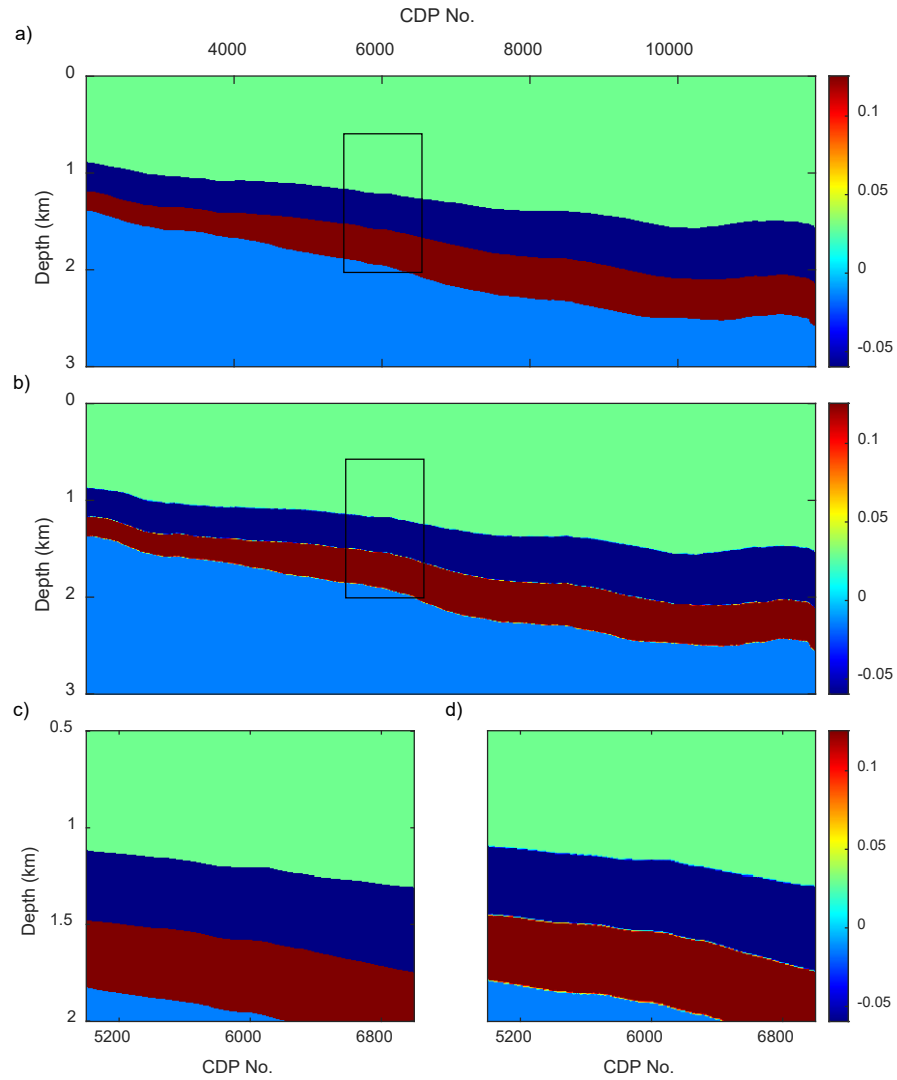


Figure 4. The  $\delta$  section (a) before tomography (initial) and (b) after tomography (updated), and (c) the initial  $\delta$  section from 0.5 to 2 km and CDP No. 5000 to 7000 and (d) updated  $\delta$  section from 0.5 to 2 km and CDP No. 5000 to 7000.

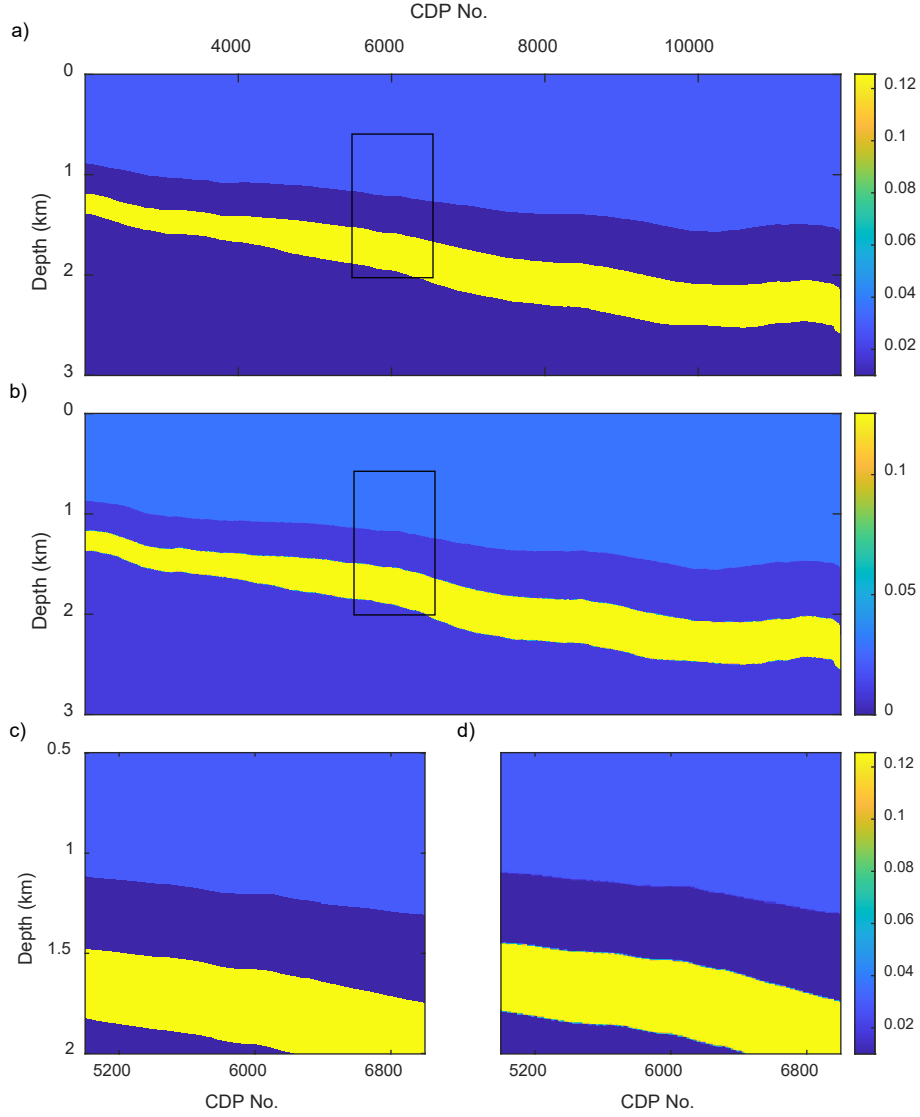


Figure 5. The  $\epsilon$  section (a) before tomography (initial) and (b) after tomography (updated), and (c) initial  $\epsilon$  section from 0.5 to 2 km and CDP No. 5000 to 7000 and (d) updated  $\epsilon$  section from 0.5 to 2 km and CDP No. 5000 to 7000.

### Comparison between isotropic PSDM and APSDM

This section presents a comparison between gathers and stacks produced with isotropic PSDM and APSDM. Regarding the gathers, upon the isotropic PSDM, events were expectedly imaged as hockey sticks due to the anisotropic nature of the medium. An example is the event appearing at a depth of 1.4 km on the gathers shown in Fig. 6a. APSDM, however, could flatten those events properly (Fig. 6b). This flattening not only increases the SNR but also strengthens the consistency of events on the stacked section. The section produced upon APSDM (Fig. 7d) shows a high SNR (*e.g.*, the events in the depth range of 0.8 to 0.9 km) coupled with strong continuity of events (*e.g.*, events in the depth range of 1 to 1.3 km and CDP No. 2400 to 2800 in Figs. 7c and 7d).



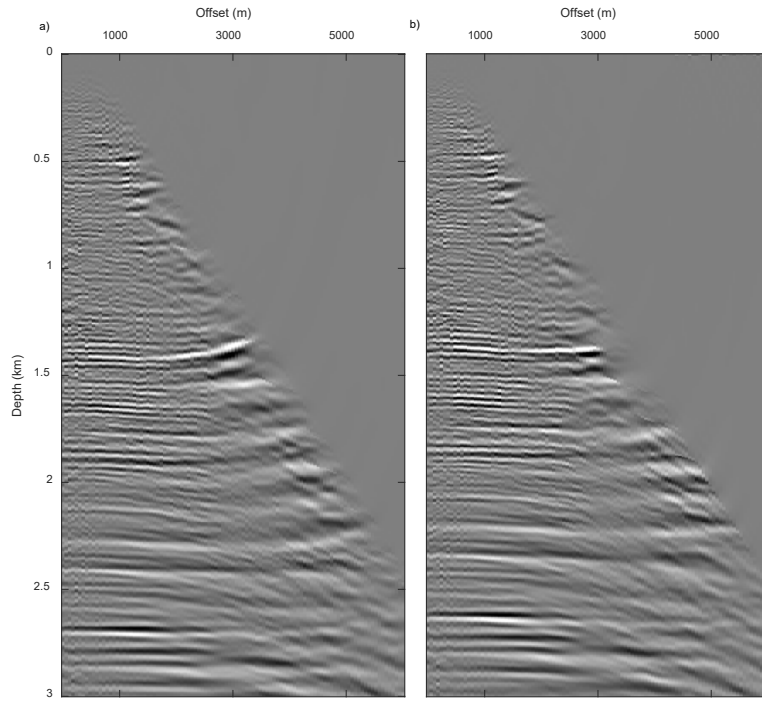


Figure 6. (a) Isotropic PSDM gathers compared to (b) APSDM gathers.

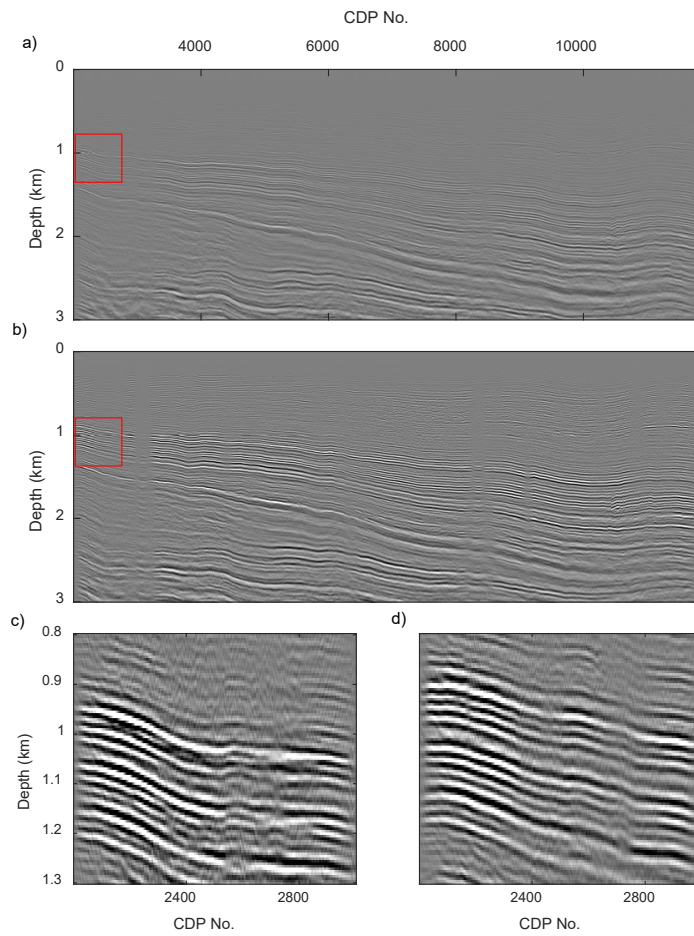


Figure 7. (a) Isotropic PSDM stacked section compared to (b) APSDM stacked section. Parts (c) and (d) demonstrate zoomed versions of isotropic PSDM and APSDM results corresponding to the depth range of 0.8 to 1.3 km and CDP range of 2002 to 3000, respectively.

## Well tops and seismic horizons

This section compares the results of isotropic PSDM and APSDM in terms of migrated horizons to the well tops along two wells (*i.e.*, AY1 and BZ1). The horizons were migrated from time to depth by the corresponding velocity model for the considered migration type (*i.e.*, isotropic and anisotropic). Figs. 8a and 8b show the depths of four seismic horizons upon isotropic PSDM and APSDM, respectively. The well tops along the Wells AY1 and BZ1 (closest to the CDP Nos. 5798 and 2807, respectively), however, give true depths of the subsurface horizons. The vertical shifts to the true depth of events due to the  $\delta$  parameter are demonstrated in Fig. 9, which leads to near-zero depth differences between the borehole markers and seismic horizons (Table 2). As shown in Fig. 9, all borehole markers along Well AY1 were shallower than the corresponding seismic horizons upon the isotropic PSDM. In contrast, APSDM could image the horizons very close to their true subsurface depths. In the absence of significant lateral heterogeneity, the values of Thomson's parameters are valid along the seismic line. Fig. 10 presents a comparison between the borehole markers along Well BZ1 (at a distance of 14955 m from the Well AY1) and the APSDM-produced seismic horizons. As reported in Table 2, upon applying APSDM rather than isotropic PSDM, the depth differences between the seismic horizons and the borehole markers decreased from 31, 35, 55, and 16 m to 4, 10, 8, and 11 m, respectively. This implies that Thomson's parameters remain valid for both wells regardless of their 15 km distance, indicating the high degree of lateral homogeneity across the study area.

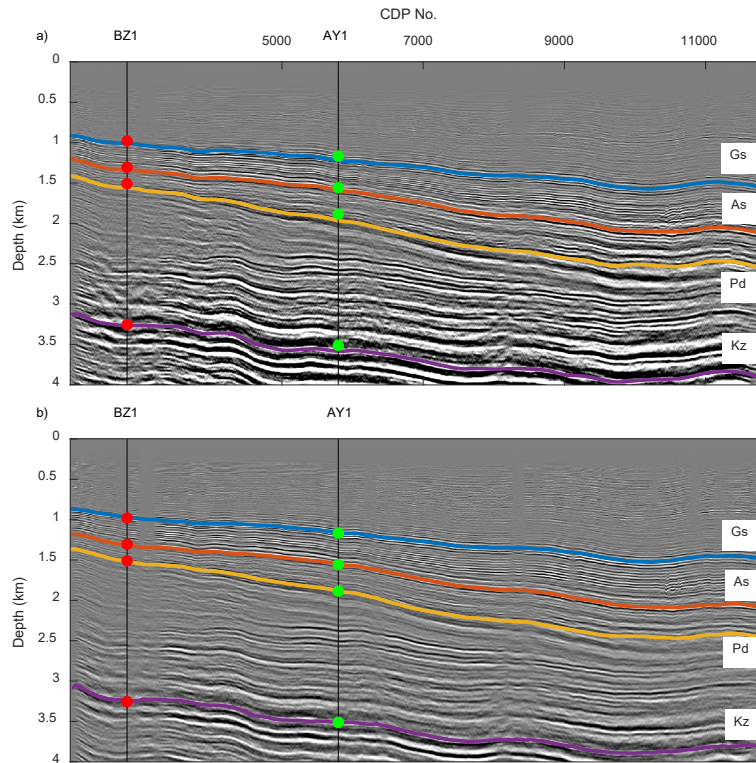


Figure 8. Stacked sections produced with (a) isotropic PSDM and (b) APSDM. Seismic horizons and borehole markers are further indicated (green dots: Well AY1; red dots: Well BZ1).

Table 2. Depth differences between borehole markers and seismic horizons.

Horizons	Well AY1		Well BZ1	
	$\Delta d_{isotropic}(m)$	$\Delta d_{anisotropic}(m)$	$\Delta d_{isotropic}(m)$	$\Delta d_{anisotropic}(m)$
Gs	56	0.5	31	4
As	37	0.5	35	10
Pd	76	0.5	55	8
Kz	72	1	15	11

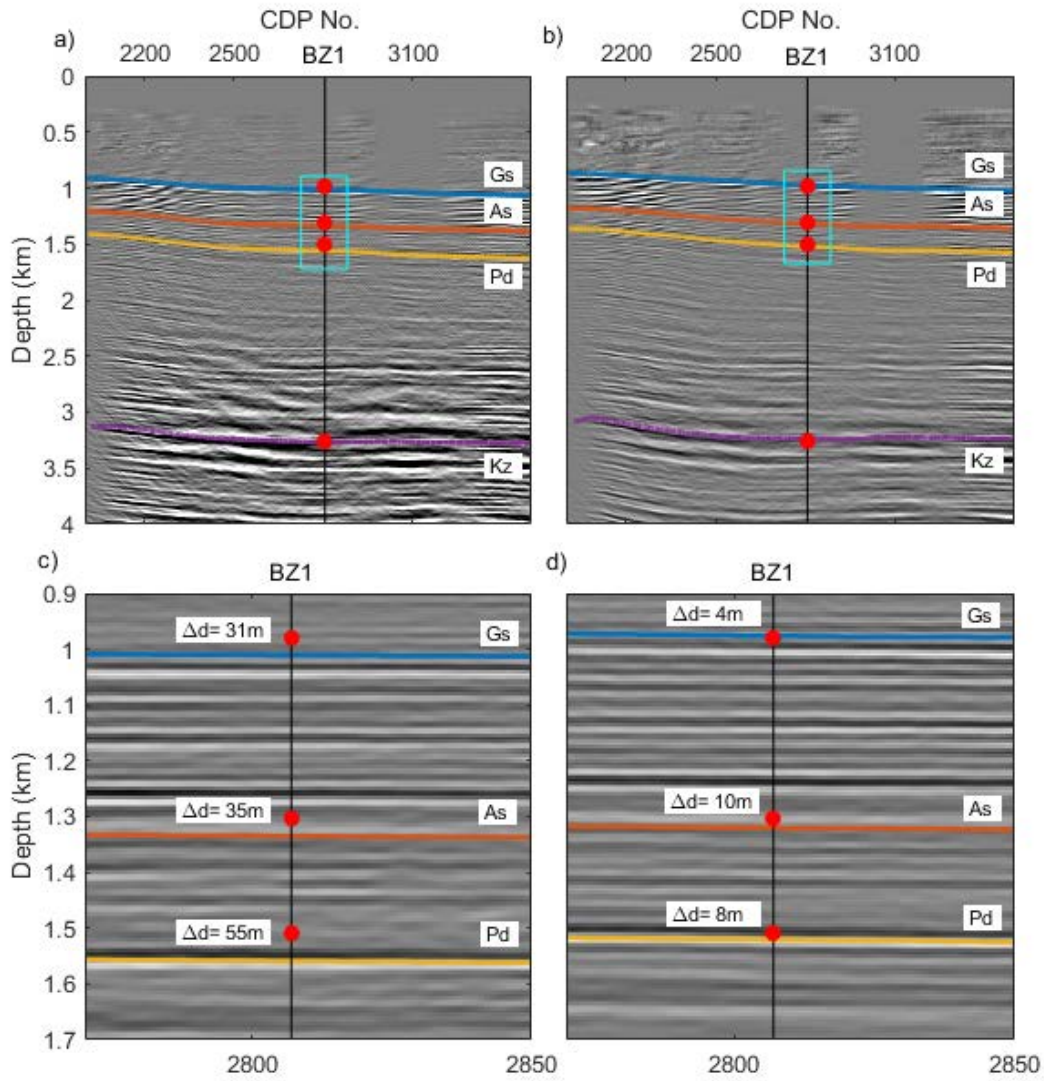


Figure 9. Windows of stacked sections produced with the help of (a, c) isotropic PSDM and (b, d) APSDM. Parts (a) and (b) correspond to a depth range of 0 to 4 km and a CDP range of 5000 to 7000, while parts (c) and (d) refer to a depth range of 1 to 2 km and a CDP range of 5600 to 6000. Seismic horizons and borehole markers along Well AY1 are further indicated.

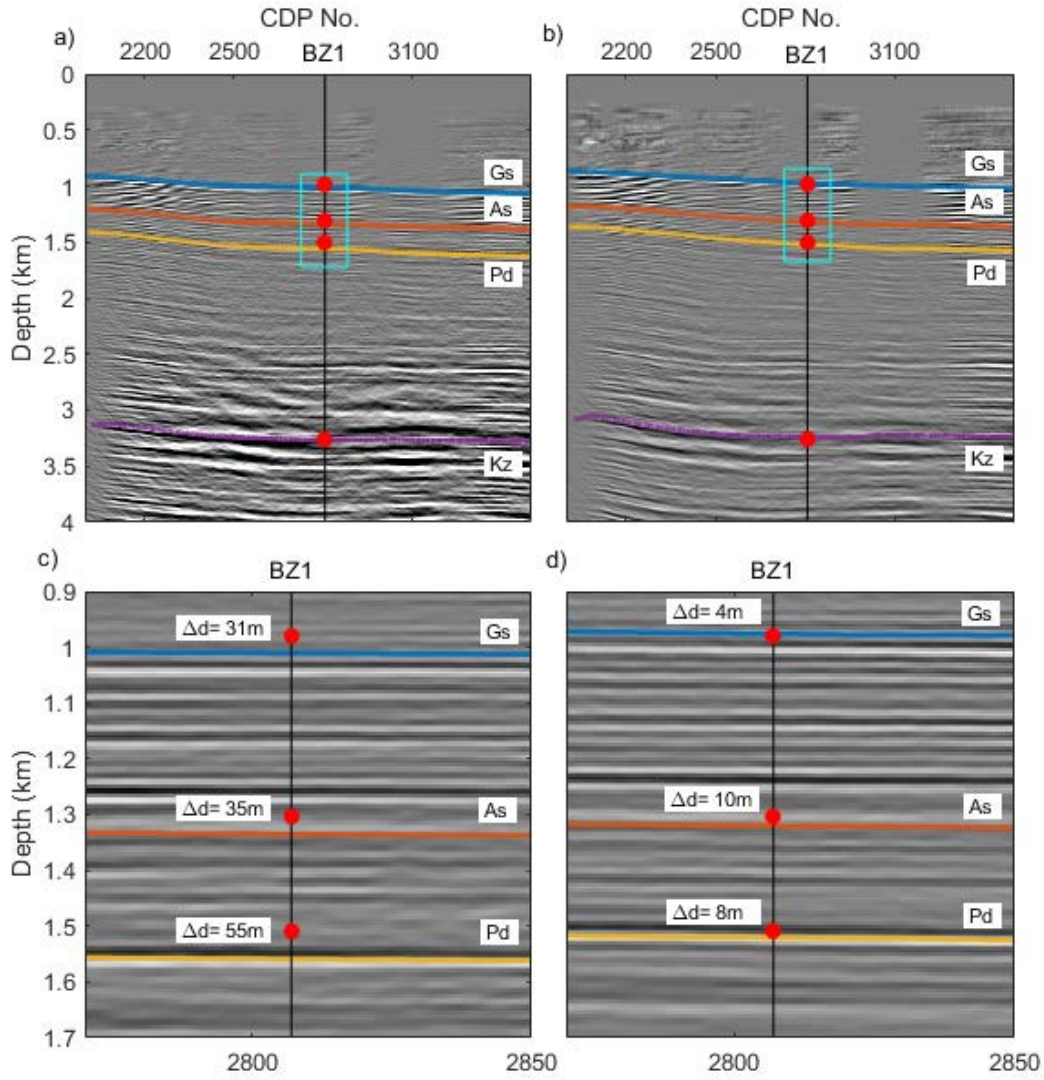


Figure 10. Windows of stacked sections produced with the help of (a, c) isotropic PSDM and (b, d) APSDM. Parts (a) and (b) correspond to a depth range of 0 to 4 km and a CDP range of 2000 to 3500, while parts (c) and (d) refer to a depth range of 0.9 to 1.7 km and a CDP range of 2770 to 2850. Seismic horizons and borehole markers along Well BZ1 are further indicated.

## CONCLUSIONS

We used APSDM to develop a realistic image of subsurface structures in Abadan Plain, southwestern Iran. Compared to isotropic PSDM, APSDM significantly improved the quality of the subsurface image in terms of reflector continuity and illuminating the seismic events. It has addressed the depth mismatch between the seismic horizons and borehole markers. In this study, the anisotropic velocity model is constructed based on the data from a borehole near the seismic profile and then validated using the data from a second borehole located at a distance of 15 km from the first borehole. The achieved match between the borehole markers along the second well and the APSDM-migrated



seismic horizons indicates that, despite its anisotropic nature, the investigated medium shows a high degree of homogeneity within individual horizons along the seismic profile.

## ACKNOWLEDGMENTS

This research did not receive any specific grant from funding agencies in the public, commercial, or not-for-profit sectors.

## DECLARATIONS

Conflict of interest: The authors declare no competing interests.

## REFERENCES

- Al-Chalabi, M. (2014). *Principles of seismic velocities and time-to-depth conversion*. Earthdoc.
- Alkhalifah, T., & Larner, K. (1994). Migration error in transversely isotropic media. *Geophysics*, 59(9), 1405-1418.
- Alkhalifah, T., & Tsvankin, I. (1995). Velocity analysis for transversely isotropic media. *Geophysics*, 60(5), 1550-1566.
- Isaac, J. H., & Lawton, D. C. (1999). Image mispositioning due to dipping TI media: A physical seismic modeling study. *Geophysics*, 64(4), 1230-1238.
- Schneider, W. A. (1978). Integral formulation for migration in two and three dimensions. *Geophysics*, 43(1), 49-76.
- Stovas, A., & Fomel, S. (2017). The modified generalized moveout approximation: A new parameter selection. *Geophysical Prospecting*, 65(3), 687-695.
- Thomsen, L. (1986). Weak elastic anisotropy. *Geophysics*, 51(10), 1954-1966.
- Thomsen, L. (2014). *Understanding seismic anisotropy in exploration and exploitation*. Society of Exploration Geophysicists.
- Tsvankin, I. (1994). P-wave signatures and parameterization of transversely isotropic media: An overview.
- Tsvankin, I., & Thomsen, L. (1994). Nonhyperbolic reflection moveout in anisotropic media. *Geophysics*, 59(8), 1290-1304.
- Vinje, V., Iversen, E., & Gjoystdal, H. (1993). Traveltime and amplitude estimation using wavefront construction. *Geophysics*, 58(8), 1157-1166.
- Yilmaz, Ö. (2001). *Seismic data analysis: Processing, inversion, and interpretation of seismic data*. Society of exploration geophysicists.